

# Computational fluid dynamics of small airway disease in chronic obstructive pulmonary disease



Yousry K. Mohamady,<sup>a</sup> Vincent Geudens,<sup>a</sup> Charlotte De Fays,<sup>a,b</sup> Marta Zapata,<sup>a</sup> Omar Hagrass,<sup>c</sup> Lucia Aversa,<sup>a</sup> Marie Vermant,<sup>a</sup> Xin Jin,<sup>a</sup> Lynn Willems,<sup>a</sup> Iwein Gyselinck,<sup>a</sup> Charlotte Hooft,<sup>a</sup> Astrid Vermaut,<sup>a</sup> Hanne Beeckmans,<sup>a</sup> Pieterjan Kerckhof,<sup>a</sup> Gitte Aerts,<sup>a</sup> Celine Aelbrecht,<sup>a</sup> Janne Verhaegen,<sup>a</sup> Andrew Higham,<sup>d</sup> Walter Coudyzer,<sup>e</sup> Emanuela E. Cortesi,<sup>a</sup> Arno Vanstapel,<sup>a</sup> John E. McDonough,<sup>f</sup> Marianne S. Carlon,<sup>a</sup> Rozenn Quarck,<sup>a</sup> Matthieu N. Boone,<sup>g</sup> Lieven Dupont,<sup>a</sup> Stephanie Everaerts,<sup>a</sup> Dirk E. Van Raemdonck,<sup>a</sup> Laurens J. Ceulemans,<sup>a,h</sup> Tillie-Louise Hackett,<sup>i</sup> Robin Vos,<sup>a</sup> Yasser Abuouf,<sup>k</sup> Joseph Jacob,<sup>l,m</sup> Wim A. Wuyts,<sup>a</sup> James C. Hogg,<sup>i</sup> Marcel Filoche,<sup>j</sup> Ghislaine Gayan-Ramirez,<sup>a</sup> Wim Janssens,<sup>a</sup> and Bart M. Vanaudenaerde<sup>a,\*</sup>

<sup>a</sup>Laboratory of Respiratory Diseases and Thoracic Surgery, BREATHE, Department of CHROMETA, KU Leuven, Leuven, Belgium

<sup>b</sup>Pneumology Lab, Institute of Experimental and Clinical Research, Université Catholique de Louvain, Brussels, Belgium

<sup>c</sup>Department of Operations Research and Financial Engineering, Princeton University, USA

<sup>d</sup>Division of Infection, Immunity and Respiratory Medicine, Faculty of Biology, Manchester University, UK

<sup>e</sup>Department of Radiology, UZ Leuven, Leuven, Belgium

<sup>f</sup>Firestone Institute for Respiratory Health, St Joseph's Healthcare Hamilton, McMaster University, Hamilton, Canada

<sup>g</sup>Dept of Physics and Astronomy, UGCT, Radiation Physics, Ghent University, Gent, Belgium

<sup>h</sup>Translational Cell and Tissue Research, KU Leuven and UZ Leuven, Leuven, Belgium

<sup>i</sup>Center for Heart Lung Innovation, The University of British Columbia, Vancouver, Canada

<sup>j</sup>Physique de la Matière Condensée, Ecole Polytechnique, Palaiseau, France

<sup>k</sup>Department of Mechanical Engineer, Alexandria University, Egypt

<sup>l</sup>Hawkes Institute, Department of Computer Science, UCL, London, UK

<sup>m</sup>UCL Respiratory, UCL, London, UK

## Summary

**Background** Small airways (<2 mm diameter) are major sites of airflow obstruction in chronic obstructive pulmonary disease (COPD). This study aimed to quantify the impact of small airway disease, characterized by narrowing, occlusion, and obliteration, on airflow parameters in smokers and end-stage patients with COPDs.

**Methods** We performed computational fluid dynamics (CFD) simulations of inspiratory airflow in three lung groups: control non-used donor lungs (no smoking/emphysema history), non-used donor lungs with a smoking history and emphysema, and explanted end-stage COPD lungs. Each group included four lungs, with two tissue cylinders. Micro-CT-scanned small airways were segmented into 3D models for CFD simulations to quantify pressure, resistance, and shear stress. CFD results were benchmarked against simplified linear and Weibel models.

**Findings** CFD simulations showed higher pressures in COPD vs. controls ( $p = 0.0091$ ) and smokers ( $p = 0.015$ ), along with increased resistance ( $p = 0.0057$  vs. controls;  $p = 0.0083$  vs. smokers) and up to a tenfold rise in shear stress ( $p = 0.010$  vs. controls). Narrowing and occlusion were shown to independently increase pressure, resistance, and shear stress, which were validated through segmentation corrections. Pressures and resistance assessed with simplified models were up to seven-fold higher for smokers and even 72 higher for COPD compared with CFD values.

eBioMedicine

2025;114: 105670

Published Online xxx

<https://doi.org/10.1016/j.ebiom.2025.105670>

1016/j.ebiom.2025.105670

105670

\*Corresponding author. Department of Chronic Diseases, and Metabolism (CHROMETA), Laboratory of Respiratory Diseases and Thoracic Surgery (BREATHE), O&N1bis, Box 706, Herestraat 49, Leuven B-3000, Belgium.

*E-mail addresses:* [Bart.Vanaudenaerde@kuleuven.be](mailto:Bart.Vanaudenaerde@kuleuven.be) (B.M. Vanaudenaerde), [yousry.mohamady@kuleuven.be](mailto:yousry.mohamady@kuleuven.be) (Y.K. Mohamady), [Vincent.Geudens@kuleuven.be](mailto:Vincent.Geudens@kuleuven.be) (V. Geudens), [charlotte.defays@saintluc.uclouvain.be](mailto:charlotte.defays@saintluc.uclouvain.be) (C. De Fays), [Marta.Zapata@kuleuven.be](mailto:Marta.Zapata@kuleuven.be) (M. Zapata), [oh2588@princeton.edu](mailto:oh2588@princeton.edu) (O. Hagrass), [Lucia.Aversa@kuleuven.be](mailto:Lucia.Aversa@kuleuven.be) (L. Aversa), [Marie.Vermant@kuleuven.be](mailto:Marie.Vermant@kuleuven.be) (M. Vermant), [Xin.Jin@kuleuven.be](mailto:Xin.Jin@kuleuven.be) (X. Jin), [Lynn.Willems@kuleuven.be](mailto:Lynn.Willems@kuleuven.be) (L. Willems), [iwein.gyselinck@uzleuven.be](mailto:iwein.gyselinck@uzleuven.be) (I. Gyselinck), [Charlotte.Hooft@kuleuven.be](mailto:Charlotte.Hooft@kuleuven.be) (C. Hooft), [Astrid.Vermaut@kuleuven.be](mailto:Astrid.Vermaut@kuleuven.be) (A. Vermaut), [Hanne.Beeckmans@kuleuven.be](mailto:Hanne.Beeckmans@kuleuven.be) (H. Beeckmans), [Pieterjan.Kerckhof@kuleuven.be](mailto:Pieterjan.Kerckhof@kuleuven.be) (P. Kerckhof), [Gitte.Aerts@kuleuven.be](mailto:Gitte.Aerts@kuleuven.be) (G. Aerts), [Celine.Aelbrecht@kuleuven.be](mailto:Celine.Aelbrecht@kuleuven.be) (C. Aelbrecht), [Janne.Verhaegen@kuleuven.be](mailto:Janne.Verhaegen@kuleuven.be) (J. Verhaegen), [andrew.higham@manchester.ac.uk](mailto:andrew.higham@manchester.ac.uk) (A. Higham), [walter.coudyzer@uzleuven.be](mailto:walter.coudyzer@uzleuven.be) (W. Coudyzer), [EmanuelaE.Cortesi@kuleuven.be](mailto:EmanuelaE.Cortesi@kuleuven.be) (E.E. Cortesi), [Arno.Vanstapel@kuleuven.be](mailto:Arno.Vanstapel@kuleuven.be) (A. Vanstapel), [jmcdonough@mcmaster.ca](mailto:jmcdonough@mcmaster.ca) (J.E. McDonough), [Marianne.Carlon@kuleuven.be](mailto:Marianne.Carlon@kuleuven.be) (M.S. Carlon), [Rozenn.Quarck@kuleuven.be](mailto:Rozenn.Quarck@kuleuven.be) (R. Quarck), [Matthieu.Boone@UGent.be](mailto:Matthieu.Boone@UGent.be) (M.N. Boone), [Lieven.dupont@uzleuven.be](mailto:Lieven.dupont@uzleuven.be) (L. Dupont), [stephanie.everaerts@uzleuven.be](mailto:stephanie.everaerts@uzleuven.be) (S. Everaerts), [dirk.vanraemdonck@uzleuven.be](mailto:dirk.vanraemdonck@uzleuven.be) (D.E. Van Raemdonck), [laurens.ceulemans@uzleuven.be](mailto:laurens.ceulemans@uzleuven.be) (L.J. Ceulemans), [Tillie.Hackett@hli.ubc.ca](mailto:Tillie.Hackett@hli.ubc.ca) (T.-L. Hackett), [Robin.Vos@uzleuven.be](mailto:Robin.Vos@uzleuven.be) (R. Vos), [yasser.abuouf@alexu.edu.eg](mailto:yasser.abuouf@alexu.edu.eg) (Y. Abuouf), [j.jacob@ucl.ac.uk](mailto:j.jacob@ucl.ac.uk) (J. Jacob), [Wim.Wuyts@uzleuven.be](mailto:Wim.Wuyts@uzleuven.be) (W.A. Wuyts), [Jim.Hogg@hli.ubc.ca](mailto:Jim.Hogg@hli.ubc.ca) (J.C. Hogg), [marcel.filoche@espci.psl.eu](mailto:marcel.filoche@espci.psl.eu) (M. Filoche), [Ghislaine.gayan-ramirez@kuleuven.be](mailto:Ghislaine.gayan-ramirez@kuleuven.be) (G. Gayan-Ramirez), [wim.janssens@uzleuven.be](mailto:wim.janssens@uzleuven.be) (W. Janssens).

**Interpretation** These findings show that increased airflow parameters can explain the association between small airway disease and airflow limitation in COPD, underscoring small airway vulnerability. Additionally, they highlight the limitations of theoretical models in accurately capturing small airway disease.

**Funding** Supported by the KU Leuven (C16/19/005).

**Copyright** © 2025 The Author(s). Published by Elsevier B.V. This is an open access article under the CC BY-NC-ND license (<http://creativecommons.org/licenses/by-nc-nd/4.0/>).

**Keywords:** Chronic obstructive pulmonary disease (COPD); Small airway disease; Computational fluid dynamics (CFD); Airway remodelling; Airway resistance; Obstruction

### Research in context

#### Evidence before this study

Studies using the retrograde catheter technique have demonstrated that small conducting airways, less than 2 mm in internal diameter, are the primary site of airflow obstruction in patients with severe chronic obstructive pulmonary disease (COPD). Subsequent investigations have established a strong association between small airway disease and lung function decline, emphasizing its critical role in COPD progression. However, these studies have primarily focused on broad clinical correlations and lack detailed insights into the underlying biomechanical mechanisms. To date, no study has explicitly simulated the interplay between airflow dynamics and small airway disease to quantify its impact on flow parameters, such as pressure, resistance, and wall shear stress, which are essential to understanding the progression of airflow limitation in COPD.

#### Added value of this study

This study introduces an approach that combines high-resolution microCT imaging and computational fluid dynamics (CFD) to provide direct evidence that small airway disease—characterized by narrowing, occlusion, and obliteration—is a major driver of increased airway pressure, resistance, and wall shear stress in smokers and patients with COPD. Our analysis identifies the direct role of specific small

airway structural abnormalities in worsening airflow dynamics, contributing to a self-perpetuating cycle of increased resistance, driving pressure, and shear rates that likely damage the airway epithelium through high wall shear stresses. Moreover, we demonstrate the limitations of simplified mathematical models, such as linear and Weibel-based models, which underestimate key airflow parameters compared to 3D CFD models, particularly in smokers and COPD patients.

#### Implications of all the available evidence

Our findings underscore the impact of small airway disease on airflow dynamics in COPD, highlighting its role in driving increased resistance, pressure, and wall shear stress. These results provide deeper insight into the interplay between small airway structural abnormalities and airflow limitations, enhancing the understanding of COPD progression. Additionally, the demonstrated limitations of traditional morphometric models emphasize the need for advanced 3D modelling approaches, such as those integrating micro-CT imaging and CFD, to accurately assess small airway disease. Future research should prioritize these methodologies to refine therapeutic strategies and improve the design of inhaled drug delivery systems targeting small airways, potentially modifying disease progression in its earlier stages.

## Introduction

Chronic Obstructive Pulmonary Disease (COPD) stands as a significant obstructive lung disease, ranked as the third leading cause of mortality.<sup>1</sup> The aetiology of COPD primarily traces back to prolonged exposure to toxic gases and particles, predominantly stemming from cigarette smoking,<sup>2</sup> which results in progressive inflammation and damage to the alveoli and alveolar ducts (emphysema), as well as obstructive changes of the peripheral conducting airways. Eventually, this results in an irreversible obstructive airflow decrease and increased airway pressure and resistance causing the lung function to decline.<sup>3</sup>

Resistance to flow through tubes, such as airways, is inversely proportional to the square of their cross-sectional area. Consequently, the large airways from

the 3rd to 5th generation, which have the smallest total cross-sectional area (2.0–2.5 cm<sup>2</sup>),<sup>4</sup> have the most significant impact on lung function.<sup>5</sup> Although small airways have a diameter less than 2 mm, their collective contribution to resistance is minimal due to the presence of about 28,000 terminal bronchioles, which results in a large total cross sectional area,<sup>6</sup> lowering their overall resistance.<sup>7</sup> As such, it was generally accepted that the primary site of airway resistance lies within central airways, with small airways contributing less than 10% to the total airway resistance under normal conditions.<sup>5</sup> For this reason, small airways are often referred to as the “silent zone” of the lung,<sup>8</sup> where disease might accumulate for many years with very little effect. Direct measurements of the distribution of resistance by Hogg et al.<sup>9</sup> showed that peripheral airway

resistance increased by a factor of four to 40 in patients with COPD, suggesting that there is significant flow obstruction and involvement of small airways in COPD. They characterised small airway disease by pathological obstructions, such as mucus plugging, which leads to partial or total occlusion of the airway lumen, as well as narrowing and obliteration of the small airways. Subsequent studies have established that small airways are the predominant site of airflow obstruction in COPD.<sup>3,10,11</sup> By use of micro-CT on fixed and dried lung samples, McDonough et al.<sup>12</sup> showed a significant loss of small airways in end-stage COPD, with only 10% of small airways remaining. They concluded that both narrowing and loss of small airways likely account for the increased resistance reported in patients with COPD.

Although structural changes in small airways, such as narrowing and loss, are linked to increased resistance and COPD progression, yet their broader impact on airflow dynamics remains unclear. Quantitative analysis of key parameters, including pressure, velocity gradients (shear rate), and particularly flow-induced shear stress along the airway wall, is still lacking. This gap has underscored the need for integrating fluid flow modelling tools, with computational fluid dynamics (CFD) being particularly valuable for simulating and quantifying these parameters. By solving the equations of fluid flow, CFD tools enable the visualization and assessment of airflow characteristics in both healthy and diseased states. However, early CFD studies<sup>13–15</sup> were constrained by the resolution of high-resolution CT (HRCT) scans, which restricted modelling to larger airways, leaving the small airways unexplored. To address this limitation, some researchers<sup>5,16</sup> adopted simplified morphometric models, such as Weibel's,<sup>4</sup> with basic flow models like Poiseuille model<sup>17</sup> to calculate airway resistance and pressure. But whether these approaches really capture the complexity and deformable nature of small airways, particularly in COPD is not certain.

This study aimed to investigate whether narrowing, occlusion, and loss of small airways significantly increases flow parameters in smokers and patients with end-stage COPD. We hypothesize that small airway disease alters airflow parameters, such as pressure, resistance, and shear stress, which may, in turn, promote further small airway disease progression. Using CFD, we simulated inspiratory flow through reconstructed small airways from lung samples of control donors, smokers, and patients with COPD, assessing changes in pressure, resistance, shear rate, and shear stress. Integrating micro-CT morphological analysis with CFD enabled us to compare airflow parameters within the same lung sample under both normal and diseased conditions, providing direct insights into the impact of small airways disease. Furthermore, as a potential support for optimization of drug delivery in COPD, the accuracy of simplified models like a linear model (derived from average micro CT dimensions) and

the Weibel-A model<sup>4</sup> to predict pressure and resistance was evaluated in comparison with the CFD results.

## Methods

### Human lung sampling, micro CT scanning and segmentation of small airways

This study included 12 lungs divided into three groups (4 lungs/group): 1) a control group consisting in donor lungs discarded for non-pulmonary reasons, 2) a smoker group of donor lungs with known smoking history and declined for transplantation due to emphysema after surgical evaluation, collapse test and confirmed by macroscopic evaluation, CT and histology, 3) a COPD group of explant lungs from patients transplanted for end-stage COPD, free of infections or confounding diseases. All groups were age, sex, and lung side matched as closely as possible. Written informed consent was obtained from patients with COPD at listing. Lung collection adhered to the McDonough et al. protocol (Fig. 1a).<sup>12</sup>

A micro CT scan with a pixel resolution of 10  $\mu\text{m}$  was performed on selected lung cylinders (two/lung, one from the upper lobe and one from the lower) using a Skyscan 1172 (Skyscan, Kontich, Belgium) to produce high-resolution images of the small airways (Fig. 1b). The selection of the cylinders was primarily based on a key criterion that for an airway tree spanning several generations, all segments must terminate in a terminal bronchiole located within a lung cylinder, with terminal bronchiole serving as the outlet for accurate CFD analysis. Semi-automated segmentation of the airway lumen within these cylinders was conducted using ITK-SNAP (Fig. 1c)<sup>18</sup> up to the terminal bronchioles, the point of transition to respiratory bronchioles, as previously described.<sup>19</sup> Micro CT images of each segmentation were analysed to quantify the terminal bronchioles and to distinguish between obstructed and non-obstructed airways. Non-obstructed terminal bronchioles allowing airflow were designated as 'outlets'. The highest small airway segment of that small airway tree was designated as the "inlet" (Fig. 1c–e).

### Geometry and computational mesh generation

The 3D small airways segmentations were further refined with 3-matic software (Materialise, Haasrode, Belgium) to enhance quality and then used to create Computer-Aided Design (CAD) models in Ansys Space Claim 2024 R1 (Ansys Inc., Canonsburg, PA) (Fig. 1d). These CAD models were analysed to quantify geometric parameters, including the number of airway branches segmented, the inlet section's cross-sectional area and perimeter, essential for setting boundary conditions and mesh generation (Supplementary Table S1). Since the airway lumen is not perfectly circular, the hydraulic diameter was calculated as an effective measure, defined as the cross sectional area divided by four times the wetted perimeter.<sup>20</sup>

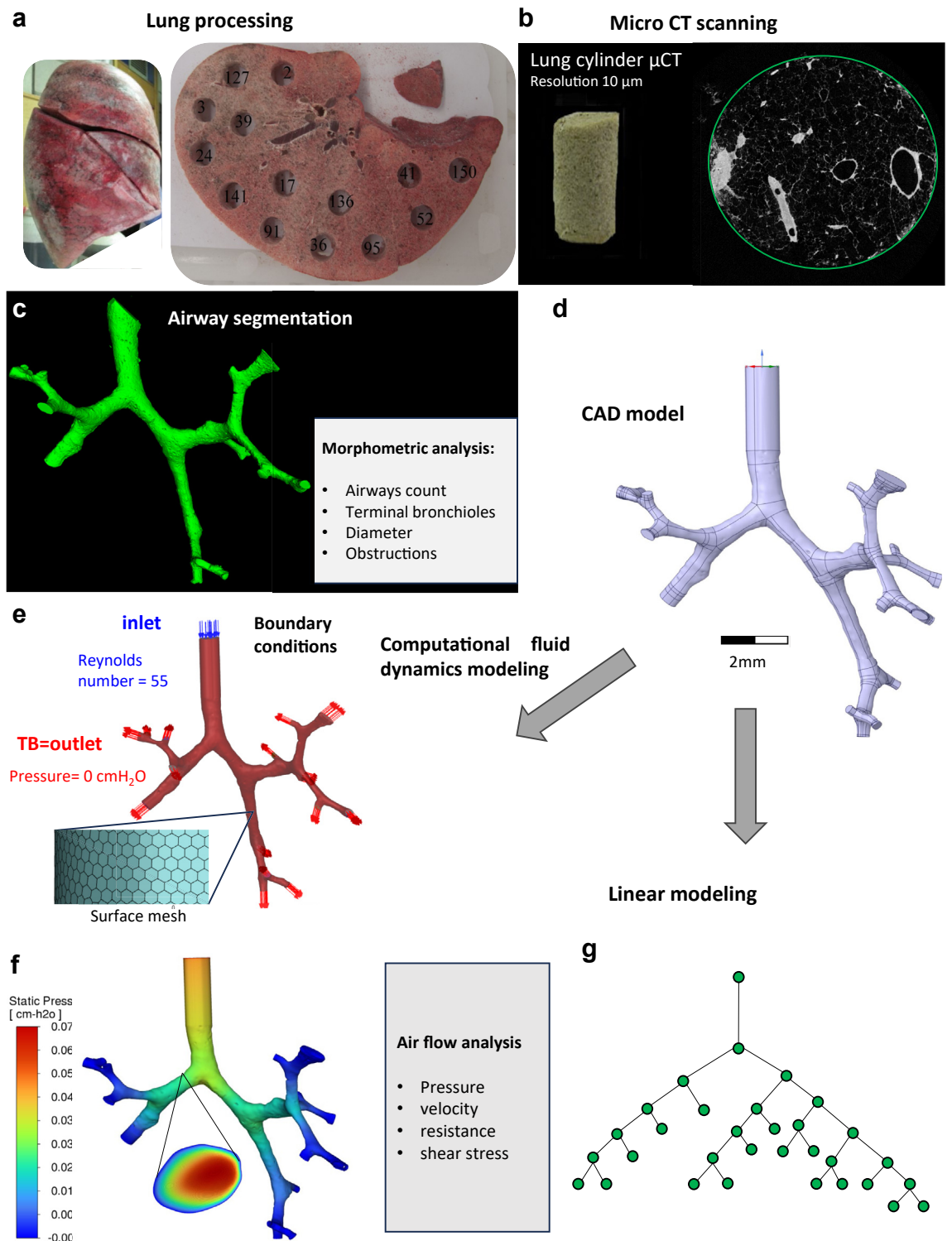


**Fig. 1:** Procedure for airflow modelling of small airways: inflated lungs (a) were sectioned into 2 cm slices, from which 2 tissue cylinders/lung with a diameter of 1.4 cm were selected. Micro-CT scans of these cylinders (b) were used to segment and analyse small airway disease. The segmented airways were further analysed (c) and converted into three-dimensional (3D) computer-aided design (CAD) models (d) for computational fluid dynamics (CFD) simulations. A computational mesh was then constructed from the CAD model (e), defining boundary

Computational grids for airflow simulations were then generated using poly-hexacore volume meshes created in Ansys Fluent Meshing 2024 R1 (Fig. 1e). These grids divided the geometry into computational cells to capture flow dynamics accurately.

### Model assumptions and boundary conditions

Inspiratory flow simulations assumed laminar, isothermal, and incompressible flow. The three-dimensional, steady-state Navier-Stokes and continuity equations for a Newtonian fluid<sup>21</sup> were solved using ANSYS Fluent 2024R1 (Ansys Inc., Canonsburg, PA). Pressure-velocity coupling was managed with the pressure implicit with splitting of operator (PISO) algorithm, and a fully implicit second-order upwind scheme was employed to solve the discretized equations.

Accurate airflow simulation requires precise boundary conditions to control air entry, exit, and wall interactions. Three boundary conditions were applied: inlet flow rate (mL/s), constant outlet pressure, and fixed no-slip walls. Due to high viscous forces in small-calibre airways, a laminar flow regime was assumed, with a baseline Reynolds number ( $Re$ ) of 55 for all inlet flows, as calculated by Nowak et al.<sup>14</sup> Consequently, the inlet velocity and flow rate was calculated from  $Re$  formula.<sup>21</sup> (Supplementary Table S2). Uniform pressure was set for all outlets, reflecting the assumption that small airways of similar size maintain similar pressure.<sup>9</sup> Convergence is defined for continuity and momentum when residuals fell below than  $10^{-6}$ .

### Assessment of small airway disease

CFD analysis was conducted to quantify changes in pressure, velocity gradients (shear rate), wall shear stress, and resistance (calculated as the pressure-to-inlet flow rate ratio) caused by specific presentations of small airway disease, such as narrowing and occlusion. To further evaluate the impact of these abnormalities, areas of airway narrowing and obstruction were reversed using segmentation software. For obstructions, the continuation of the airway beyond the blockage was identified on micro-CT images, enabling the reconnection of obliterated sections to the airway tree. This approach allowed direct comparisons of flow parameters within the same core under both obstructed and unobstructed conditions.

### Linear modelling of small airways

Airway resistance and pressure between CFD findings and simplified small airway models were compared on one representative core from each group. The first simplified model is derived from the 3D-CAD models (Fig. 1d) where a simplified 'node and segment'

structure was created, with each line representing a branch and each node indicating a bifurcation point (Fig. 1g). Average diameter and length were assigned to each branch, allowing airflow simulation using the Poiseuille equation,<sup>17</sup> implemented in C++, for calculating pressure difference and resistance. This model, where airway dimensions are derived directly from micro-CT scans, is referred to as the 'linear' model. The second simplified model, based on the Weibel-A model,<sup>4</sup> assigned uniform diameters and lengths to airway branches within each generation. To illustrate these differences, we plotted branch diameters from both simplified models for each group.

### Statistics

Statistics were conducted using Prism 10 (GraphPad, USA). Normality was assessed with the D'Agostino and Pearson tests, and results are expressed as mean ( $\pm$ SEM). Group comparisons were made using one-way ANOVA, followed by Tukey's multiple comparisons post-hoc test.  $p$ -values less than 0.05 were considered significant.

### Ethics

This study was approved by the Ethical Committee UZ Leuven (S52174/S63978). Donor lung collection followed Belgian law's opt-out system, allowing use for research if deemed unsuitable for transplant.

### Role of funders

Funders had no active role in this research or the writing of this manuscript.

## Results

### Patient characteristics and small airway morphometrics

Patient characteristics and small airway segmentation data from lung cylinders are presented in Table 1. There were no differences in age, height, and weight between the groups. Small airway was significantly reduced by 53% in patients with COPD compared to controls ( $p = 0.024$ ). Similarly, the number of outlets decreased by 47% ( $p = 0.014$ ), and the hydraulic diameter by 63% ( $p = 0.038$ ). No significant morphological changes were found in smokers compared to other groups.

### Fluid dynamics of control, smoker and COPD small airways

Inspiratory flow simulations showed a five-to sevenfold increase in pressure in small airways of the COPD group ( $1.43 \pm 0.84$  cm H<sub>2</sub>O) compared to the smoker ( $0.28 \pm 0.10$  cm H<sub>2</sub>O;  $p = 0.015$ ) and control group

conditions for the inlet and terminal (outlet) branches. CFD simulations (f) quantified flow parameters, including pressure, velocity, and shear stress within the small airways. (g) Simplified linear models, including the Weibel symmetrical model, were derived from the CAD models by assigning micro-CT-based diameters and lengths to each airway branch for airflow simulation. For the Weibel symmetrical model, the number of branches per model was maintained, while the length, diameter, and symmetry were aligned with Weibel data.

	Control	Smoker	COPD	p-value
Number of patients/lungs	4	4	4	
Number of cores	8	8	8	
Sex (Male/Female)	3/1	3/1	3/1	1.00
Age (years)	65 ± 6	48 ± 62	58 ± 4	0.21
Height (cm)	166 ± 1	176 ± 5	167 ± 3	0.19
Weight (kg)	72 ± 5	78 ± 97	55 ± 47	0.11
Nonsmoker/former/smoker(n)	4/0/0	0/0/4	0/4/0	<0.005
Smoking history (pack years)	NA	All active smoking	26 ± 11	
<b>Lung function</b>				
FEV <sub>1</sub> (%pred)	NA	NA	31 ± 3	
FVC (%pred)	NA	NA	70 ± 5	
FEV <sub>1</sub> /FVC (%pred)	NA	NA	36 ± 5	
TLC (%pred)	NA	NA	118 ± 3	
DLCO (%pred)	NA	NA	38 ± 1	
<b>HRCT ex vivo</b>				
Left/right (n)	2/2	1/3	2/2	0.41
Explant lung volume(l)	2.8 ± 0.3	3.4 ± 0.2	3.4 ± 0.4	0.42
Lung density (g/l)	97 ± 3	93 ± 9	98 ± 2	0.89
Total airways	180 ± 45	144 ± 28	130 ± 3	0.38
% emphysema score	<1	10 ± 5	57 ± 8	<0.005
<b>Small airway characteristics</b>				
Inlet diameter	1.2 ± 0.1	1.0 ± 0.1	0.7 ± 0.1	<b>0.037</b>
Number of segments	22.6 ± 2.6	18.3 ± 2.9	12.0 ± 1.8	<b>0.031</b>
Number of outlets	11.8 ± 1.4	9.6 ± 1.4	5.5 ± 1.1	<b>0.017</b>
Number of generations	5.6 ± 0.3	5.3 ± 0.3	4.3 ± 0.3	<b>0.027</b>

COPD: chronic obstructive pulmonary disease. GOLD: global initiative for chronic obstructive pulmonary disease. FEV<sub>1</sub>: forced expiratory volume in 1 s. FVC: forced vital capacity post-bronchodilator. FVC: Forced vital capacity. DLCO: diffusing lung capacity for carbon monoxide. NA: not available. HRCT: high resolution computer tomography. %pred: percentage of predicted value. Bold values indicate statistical significance (p < 0.05).

**Table 1: Patient characteristics and data on small airway segmentation: Values are given as mean ± standard error of the mean (SEM).**

(0.19 ± 0.05 cm H<sub>2</sub>O; p = 0.009), respectively (Fig. 2a–d). Small airway resistance was elevated in COPD (2.75 ± 1.56 cmH<sub>2</sub>O.sec/mL) vs. the smoker (0.41 ± 0.10 cmH<sub>2</sub>O.sec/mL; p = 0.0082) and control group (0.25 ± 0.10 cmH<sub>2</sub>O.sec/mL; p = 0.0047) (Fig. 2b). The maximum shear stress on the airway wall in the COPD group (0.24 ± 0.11 cm H<sub>2</sub>O) significantly increased fourfold vs. the control group (0.06 ± 0.02 cm H<sub>2</sub>O; p = 0.01) (Fig. 2c–e). No significant differences in pressure, resistance, and shear stress were observed between smokers and controls.

### Fluid dynamics of small airway of narrowing and occlusion

The widespread narrowing, occlusion, and loss of small airways in COPD and, to a lesser extent, in smoker cores made it challenging to isolate the effects of specific abnormalities. To address this, we systematically corrected airway models to a presumed healthy state, enabling direct comparisons of flow parameters between diseased and unobstructed conditions. This approach was applied across cases of narrowing, localized occlusion, and more severe obstructions.

An example of narrowing in a COPD cylinder showed a reduction in the hydraulic diameter of the inlet branch from 0.53 mm to 0.26 mm (Fig. 3a and b). Under the same flow conditions, the narrowed model required more than double the driving pressure and resistance of the corrected version, reaching 1.07 cm H<sub>2</sub>O and 2.42 cm H<sub>2</sub>O.s/mL, respectively (Fig. 3c). Velocity and velocity gradients increased sharply at the narrowing site (Fig. 3d), and wall shear stress more than doubled (Fig. 3e; see also Supplementary Video S1). Occlusion observed in a COPD cylinder, where airflow was completely blocked within a branch (Fig. 4a) showed that compared to a restored version with unobstructed airflow (Fig. 4b), the pressure and resistance more than doubled to sustain the same flow rate in the occluded model (Fig. 4c–e). Maximum shear stress on the airway wall tripled, rising from 0.20 cm H<sub>2</sub>O to 0.61 cm H<sub>2</sub>O (Fig. 4d and e, see also Supplementary Video S2). In a smoker's cylinder with three distinct occlusions present in small airways preceding the terminal bronchioles (Fig. 5a), a fully functional model without obstructions (Model I) was first developed in which occlusions were progressively reintroduced, leading to a series of models representing increasing severity according to the number of obstructions (Fig. 5b). Each obstruction resulted in a marked increase in pressure and airway resistance. Pressure increased from a baseline of 0.27 cm H<sub>2</sub>O in the unobstructed model to 1.50 cm H<sub>2</sub>O in the fully obstructed state, while resistance rose from 0.27 cm H<sub>2</sub>O.s/mL to 1.50 cm H<sub>2</sub>O.s/mL. Additionally, shear stress increased eightfold in the most obstructed state (Fig. 5c–e). Fig. 5c, display the corresponding pressure and wall shear stress contours, respectively, see also Supplementary Video S3). Multiple obstructions and narrowing were also observed in another smoker's airway cylinder, where the small airway exhibited narrowing and bending due to complete occlusion in an adjacent larger airway (Supplementary Fig. S1). In the most severe cases of small airway disease in COPD cylinders, total obliteration of all small airways was evident, leaving no functional airways and preventing CFD simulations (Supplementary Fig. S2).

### Comparing CFD simulations with linear and weibel-based models of small airways

The average diameters of small airways from micro-CT scans were compared with those from the Weibel-A model for the same generations (Fig. 6a).

In control cores, 3D simulations showed approximately twice the pressure and resistance values of the linear and Weibel models, which produced similar results. For smokers, 3D simulations showed two-and-a-half times higher pressure and resistance than the linear model and seven times higher than the Weibel model. The largest differences were observed in COPD cores, where 3D simulations showed pressure and resistance values five times higher than the linear model

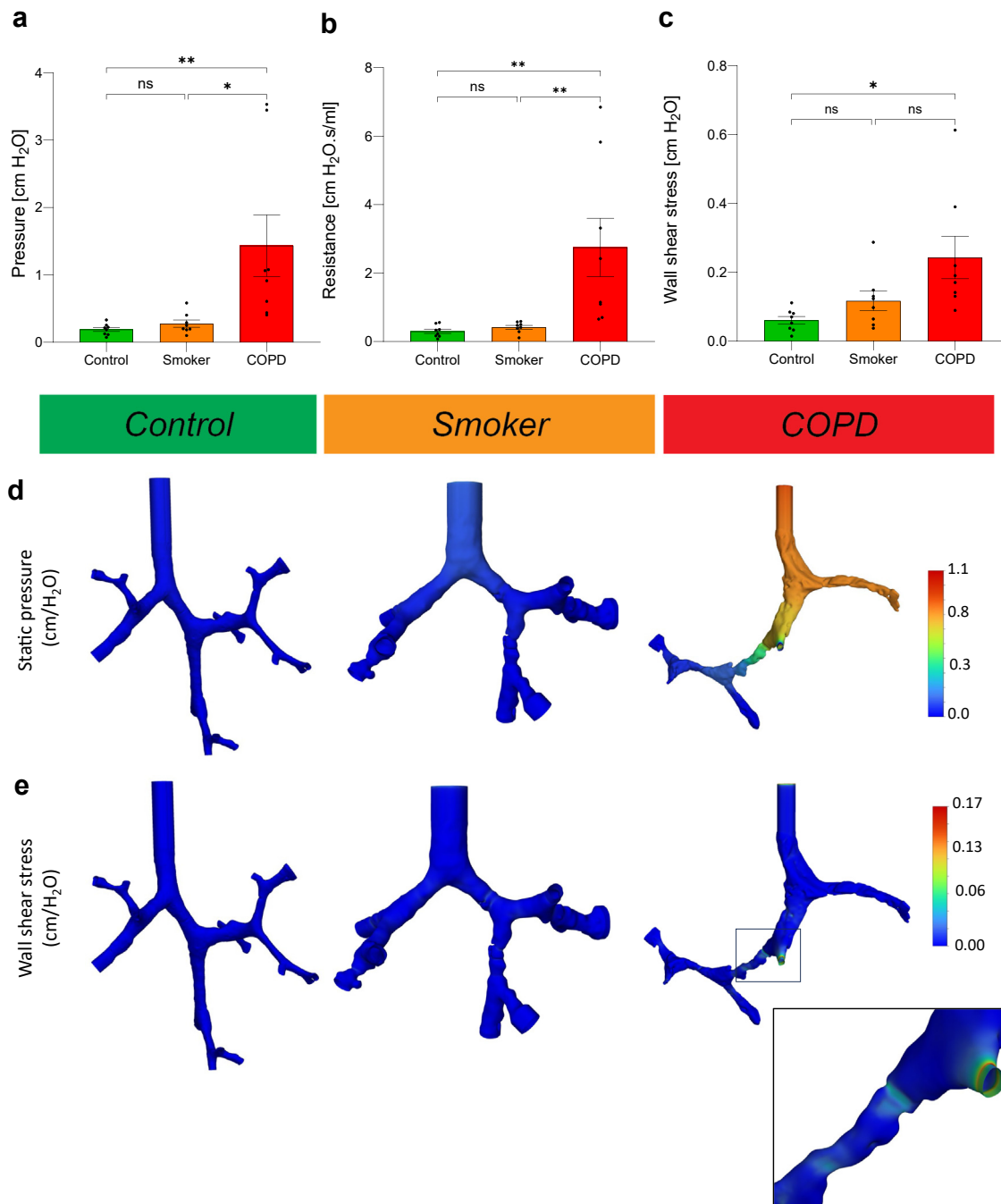


**Fig. 2:** Comparison of inlet air pressure (a), total small airway resistance (b), and wall shear stress (c) across controls, smokers, and COPD groups. ANOVA showed significant increases in airway pressure ( $p = 0.015^*$  and  $p = 0.009^{**}$ , respectively) and small airway resistance ( $p = 0.0082^{**}$  and  $p = 0.0047^{**}$ , respectively) in the COPD group compared to smokers and controls. Wall shear stress was significantly higher in the COPD group compared to controls ( $p = 0.01^*$ ). No significant differences were observed between smokers and controls for any parameter ( $p > 0.05$ ). Data represents statistical comparisons ( $n = 8$  per group). Small airways from each group are shown, visualizing pressure (d) and wall shear stress contours (e).

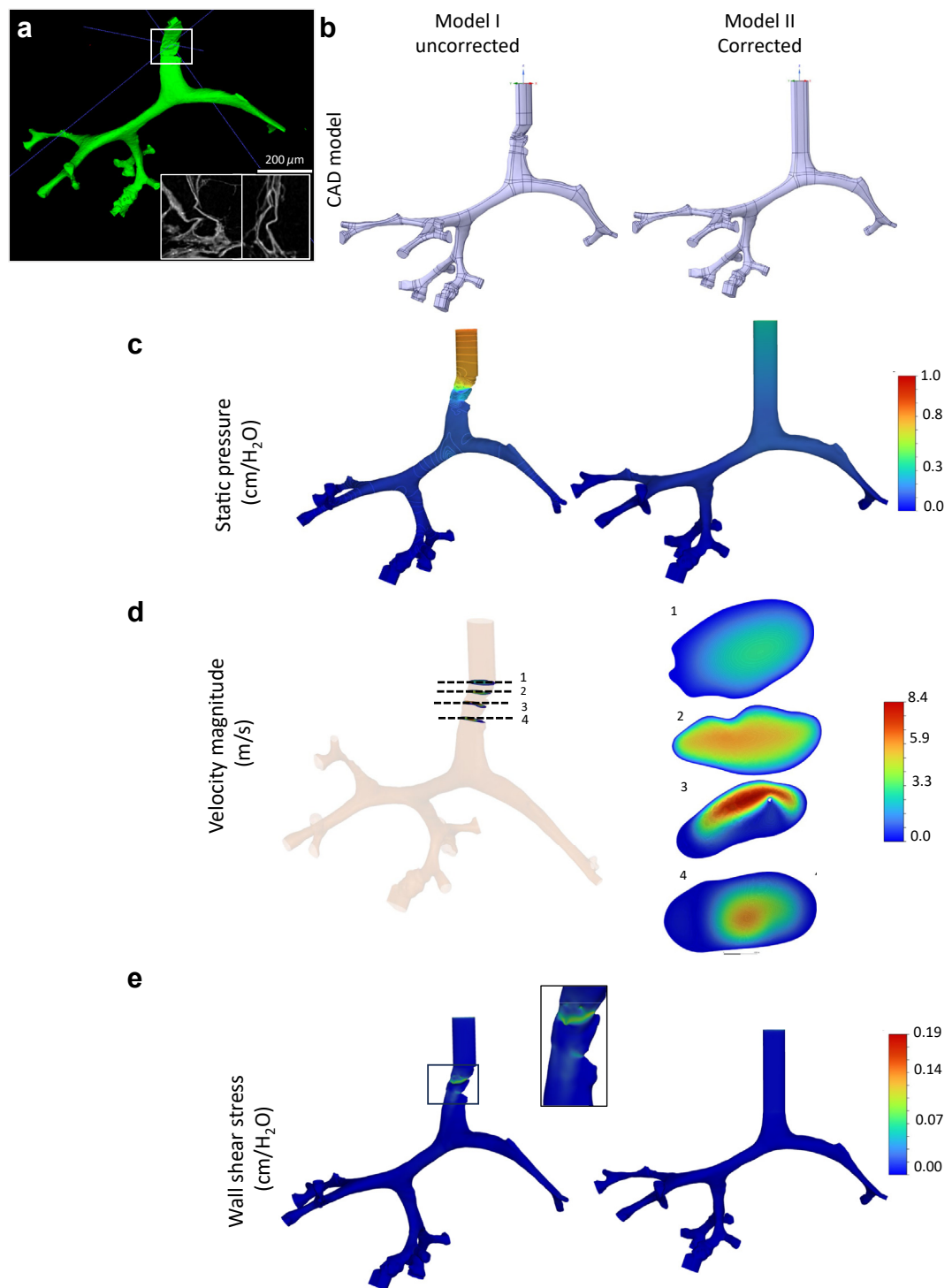


**Fig. 3: CFD simulation of an airway narrowing.** A segmentation of small airways from a COPD lung with a narrowing at the generation of the inlet (a). A CAD model was generated (model I) together with a corrected model where the narrowing was removed (model II) (b). Pressure contours (c) are illustrated for the narrowed and corrected models. Velocity contours and gradients of sequential cross-sections highlight the velocity gradients around the narrowed region (d). Wall shear stress contours (e) with magnification on the constricted region to highlight the impact of increased velocity gradients.

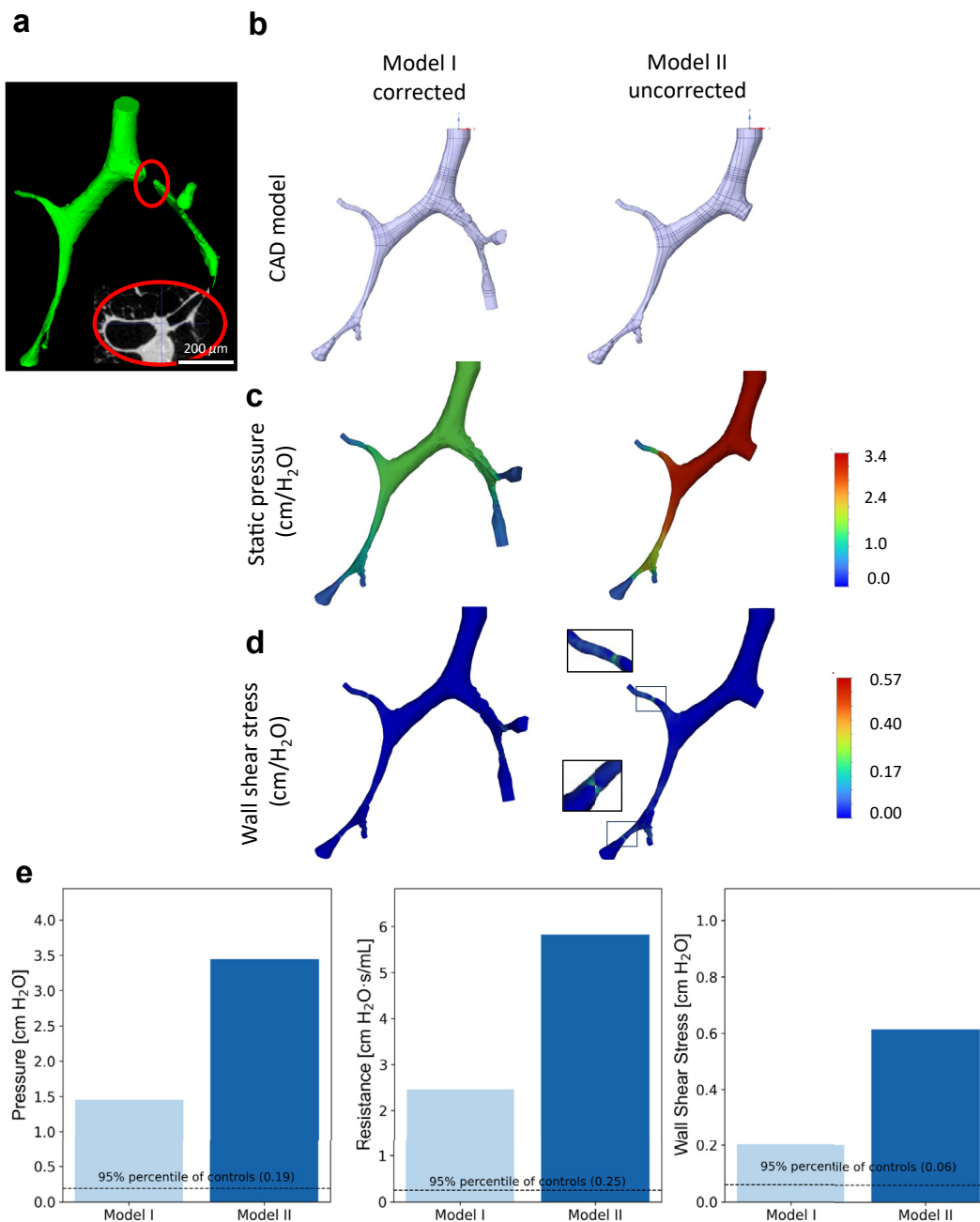


**Fig. 4:** CFD simulation of a small airway occlusion. A segmentation of a small airway with an occlusion at one generation down from the inlet branch marked by a red circle and a detailed microCT image is the accompanying red circle originating from a COPD lung (a). An uncorrected (model I) and corrected (model II) CAD model for this occlusion were generated (b) to illustrate and quantify the impact on pressure (c, e), wall shear stress (d, e), and resistance (e).

and seventy-two times higher than the Weibel model (Fig. 6b and c). This trend of increasing deviation between the 3D CFD simulations and the simplified models persisted across all generations and groups (Supplementary Fig. S3).

## Discussion

This study highlights the critical interplay between small airway disease and airflow dynamics. CFD simulated the inspiratory flow within small airways, capturing changes in flow parameters due to small airway disease, including

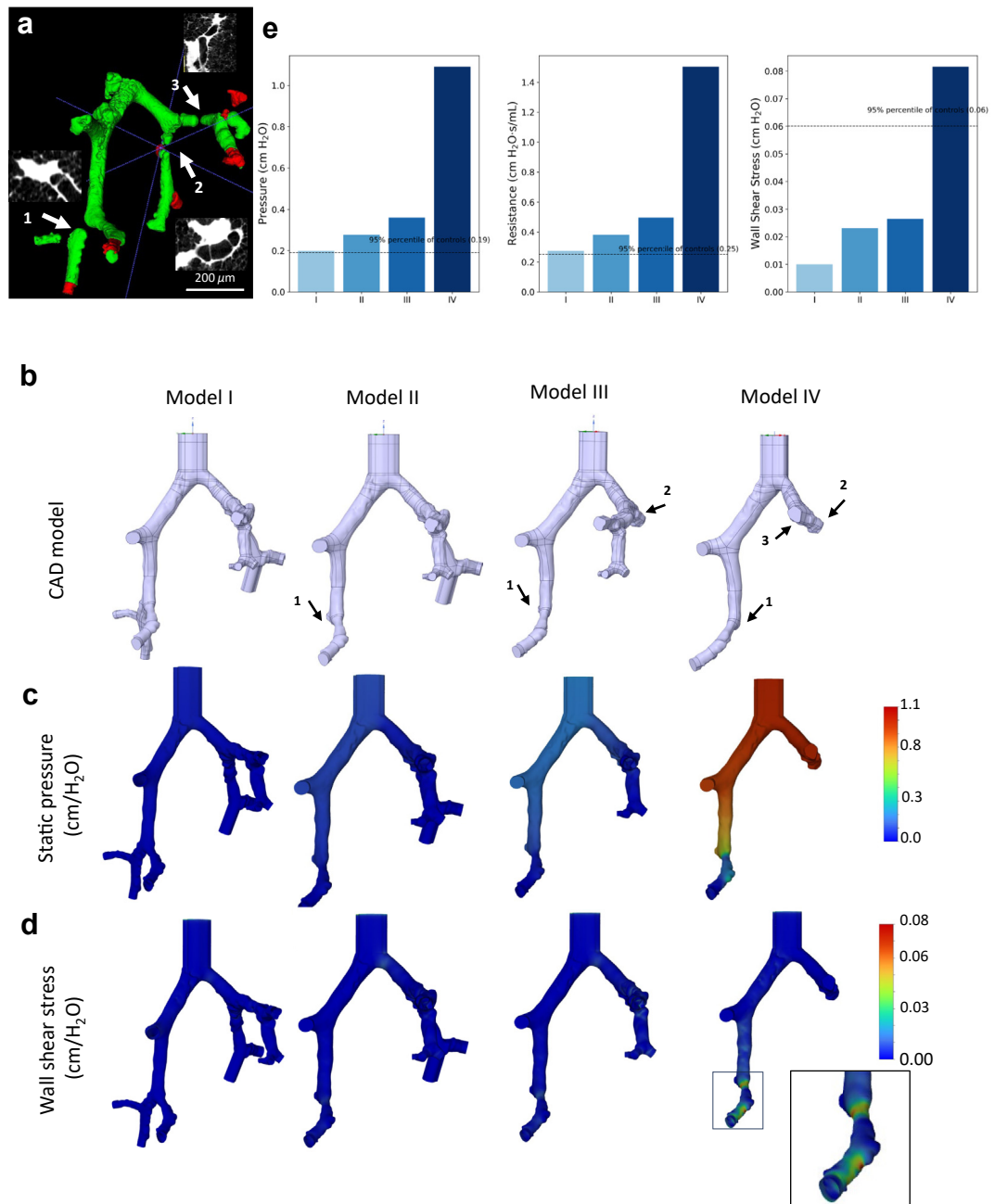


**Fig. 5: CFD simulation of multiple occlusions.** A small airway segmentation from a smoker lung included three occlusions marked by white arrows (a). CAD models (b) from the uncorrected (model IV) to the fully corrected model (model I) were used for CFD simulation. Contours of pressure (c) and wall shear stress (d) visualizing the impact of progression of small airway disease. Quantification of pressure, wall shear stress, and resistance demonstrated the impact of the multiple occlusions (e).

narrowing and occlusion. These alterations led to increases in pressure, resistance, and wall shear stress. Already within smokers, subtle changes have had an impact on airflow dynamics and may contribute to disease onset and progression. Within COPD, small airway disease substantially compromises airflow parameters,

explaining the association with airflow limitation. This study also emphasized that realistic three-dimensional simulation of small airways and not simplified linear and symmetrical models with average diameters, length and number of airway branches, are essential to evaluate the impact on airflow dynamics of small airways.

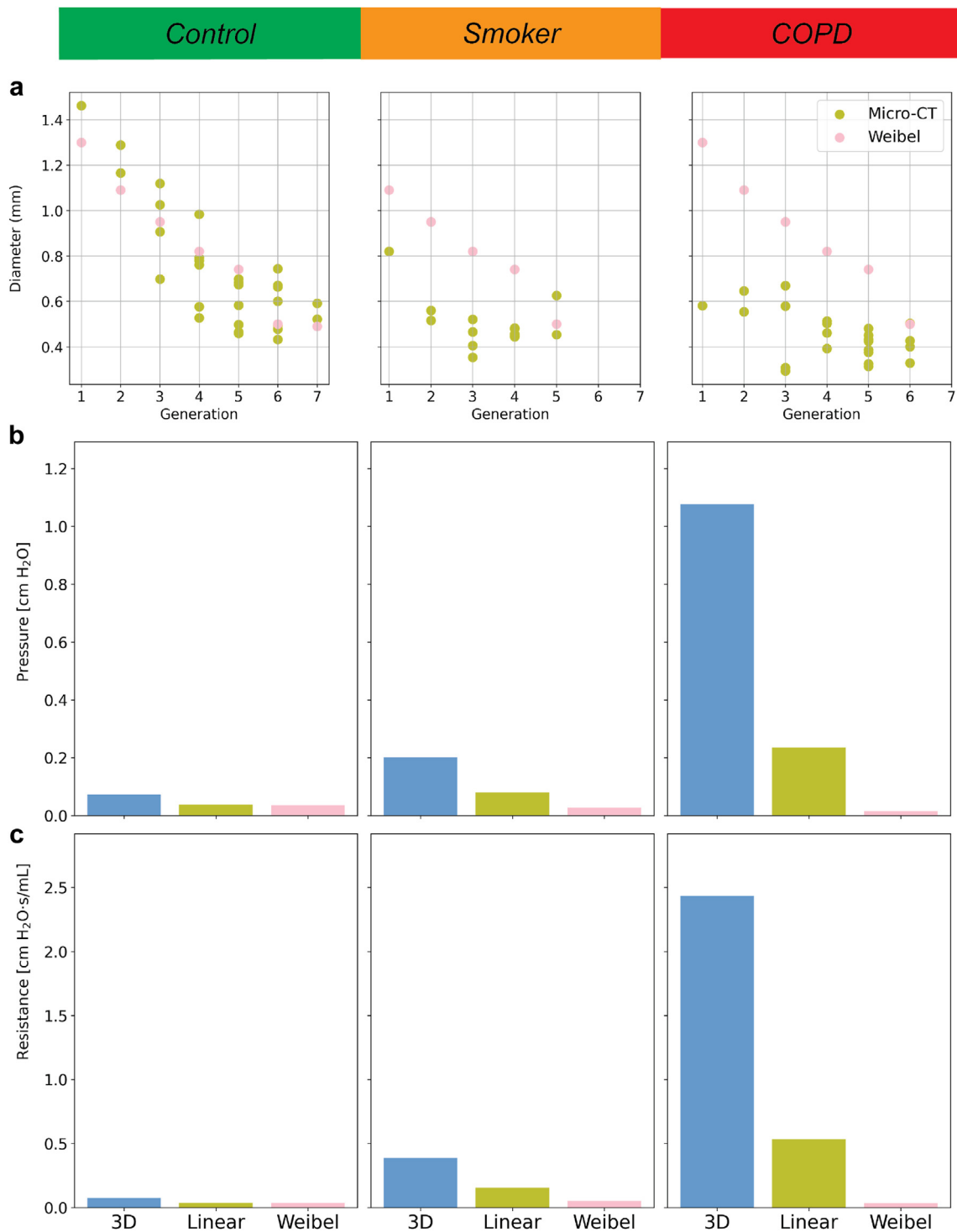


**Fig. 6:** Comparative analysis of the diverse computational models of small airways: (a) Comparison of small airway diameters derived from micro-CT with corresponding Weibel-A model values across different generations in control, smoker, and COPD samples, based on a representative core from each group (b) Pressure and (c) resistance comparison between the 3D, linear, and Weibel models for control, smoker, and COPD airways.

Our results support and extend earlier studies<sup>9–11</sup> that used the retrograde catheter technique to measure small airways resistance, providing new quantitative evidence that small airway disease is a primary cause of increased pressure, and wall shear stress in end-stage COPD. Furthermore, a significant reduction in small bronchioles along with widespread narrowing in COPD samples compared to controls were observed consistent with previous reports.<sup>12</sup> In smoker lungs, there were no significant morphological alterations compared to controls, but simulation of two smoker small airways revealed significant increases in airflow attributed to small airway disease. These findings support the hypothesis that small airways may represent one of the earliest sites of airflow limitation, emphasises the significance of early detection and intervention in COPD. In the early stages of COPD, peripheral resistance can increase with minimal impact on total lung resistance,<sup>9</sup> suggesting that patients may exhibit normal lung function despite substantial small airway disease. A previous study<sup>22</sup> has indeed shown that even in mild COPD, patients may have already lost approximately 56% of their terminal bronchioles.

The relative importance of small airway disease in lung function decline has been widely debated. In this study, we provided direct evidence that small airway disease is a primary factor in increasing airway resistance, driving pressure, and wall shear stress in COPD. Furthermore, these findings offer insight into how elevated resistance, pressure, and shear stress in small airways may contribute to airflow limitation in COPD. This can be demonstrated by considering airflow through typical bronchial bifurcations. In a scenario where one branch becomes totally occluded, airflow would be redirected entirely through the remaining open branch. Although resistance in the open branch remains constant due to unchanged dimensions, the increased flow rate necessitates a higher driving pressure to maintain airflow, as this pressure difference depends on the product of airway resistance and flow rate. This effect was particularly evident in one smoker sample, where gradually losing small airways alone contributed to elevated driving pressures. In COPD and severe emphysema, the disappearance of a large number of small bronchioles buffers a downward shift in small airways diameter.<sup>23</sup> Since resistance is inversely proportional to the fourth power of airway diameter, even minor reductions in diameter require much higher driving pressures to sustain airflow.<sup>5</sup> This process also drives marked increases in wall shear stress, which rises proportionally with both shear rate and pressure. Our analysis revealed that shear stress levels in COPD were ten times higher than in controls and five times higher than in smokers. These findings align with Nucci et al.,<sup>24</sup> who observed that airway constriction can significantly amplify shear stress, potentially increasing it up to 50-fold in severe chronic conditions. These elevated

shear stress levels can initiate a cascade of tissue responses, including inflammation, tissue damage, and progressive airway remodelling.<sup>24–26</sup> A key example of this stress response is connective tissue formation at the epithelial interface as an immune-mediated protective mechanism against shear stress.<sup>27,28</sup> Considering that a substantial amount of conducting small airways become lost or narrowed, the remaining functional airways increasingly struggle to maintain normal ventilation. This deterioration initiates a self-perpetuating cycle: higher resistance demands supraphysiological pressures for ventilation, which in turn elevate shear stress and accelerate small airway disease. These processes, compounded by emphysema and the loss of alveolar attachment, contribute to COPD progression and lung function decline.<sup>29,30</sup> This analysis aligns with established findings that COPD progression is associated with airway wall thickening, lumen narrowing and loss of small airways.<sup>3,22</sup>

This study also emphasizes the importance of realistic morphometric models for studying airflow dynamics within small airways, particularly in diseased states. Nowak et al.<sup>14</sup> previously highlighted this need in larger airways when investigating particle deposition for drug delivery, showing that the Weibel model-A fails to capture the complexity of airflow compared to CT-based models. Similarly, our comparative analysis of measurements based on micro CT-based, linear, and Weibel geometries reveals that simplified models, though adequate for healthy lungs morphometry, produce significant inaccuracies in diseased conditions. In smokers, subtle airway narrowing and deformation lead to underestimation of pressure and resistance, while in COPD, severe pathological changes further exacerbate these inaccuracies. The primary reason for the failure of simplified models is their inability to capture the structural changes of small airways, which can only be achieved through micro-CT imaging.

In conclusion, the increased driving pressure and shear stress resulting from elevated resistance due to small airway disease likely add to the progress of small airway disease and early airflow limitation in COPD, and perhaps even prior to measurable declines in lung function. Importantly, our study emphasizes the limitations of simplified airway models and highlights the need to consider reliable model based on micro-CT that reveals small airway disease in future research, especially in the design of inhaled drug delivery therapies for COPD treatment.

### Limitations

This study focused on airflow in small airways to emphasize their critical role in COPD. While this approach highlights the impact of small airway disease, future research should examine the entire airway tree to better understand lung physiology, particularly interactions between small and large airways during

ventilation. Achieving this will require next-generation imaging tools capable of high-resolution scans of the entire lung.

The cross-sectional nature of this study limits insights into the temporal evolution of airflow dynamics and their long-term effects. Although our steady-state simulations at total lung capacity (TLC) during inspiration provide valuable data, future studies should incorporate time-dependent simulations with actual lung function measurements. Incorporating a fluid–structure interaction (FSI) model could further clarify how airway wall mechanics respond to elevated flow parameters.

Additionally, the relatively small sample size limits generalizability, though the selected samples were appropriate for investigating COPD progression. Despite this limitation, distinct effects were observed, and our CFD results align with previous reports of increased peripheral airway resistance in COPD compared to normal values.

#### Contributors

Yousry K. Mohamady: Resources, running simulations, data curation, writing—original draft, writing original codes for the linear ventilation program, validation, review & editing.

Vincent Geudens: Resources, data curation, validation, review & editing.

Charlotte De Fays: Resources, data curation, validation, review & editing.

Marta Zapata: Resources.

Omar Hagrass: Validation, review & editing.

Lucia Aversa: Resources, review & editing.

Marie Vermant: Resources, review & editing.

Xin Jin: Resources, review & editing.

Lynn Willems: Resources, review & editing.

Iwein Gyselinck: Resources, review & editing.

Charlotte Hoof: Resources, review & editing.

Astrid Vermaut: Resources, review & editing.

Hanne Beeckmans: Resources, review & editing.

Pieterjan Kerckhof: Resources.

Gitte Aerts: Resources.

Celine Aelbrecht: Resources.

Janne Verhaegen: Resources, review & editing.

Andrew Higham: Resources, review & editing.

Walter Coudyzer: Resources.

Emanuela E. Cortesi: Resources, review & editing.

Arno Vanstapel: Resources, review & editing.

John E. McDonough: Resources, validation, review & editing.

Marianne S. Carlon: Resources, validation, review & editing.

Rozenn Quarck: Resources, review & editing.

Matthieu N. Boone: Resources.

Lieven Dupont: Resources.

Stephanie Everaerts: Validation, review & editing.

Dirk E. Van Raemdonck: Resources, review & editing.

Laurens J. Ceulemans: Resources, validation, review & editing.

Tillie-Louise Hackett: Resources, review & editing.

Robin Vos: Resources, validation, review & editing.

Yasser Abuouf: Validation, review & editing.

Joseph Jacob: Resources, review & editing.

Wim A. Wuyts: Resources, review & editing, supervision.

James C. Hogg: Resources, review & editing.

Marcel Filoche: Supervision, validation, review & editing.

Ghislaine Gayan-Ramirez: Supervision, resources, validation, review & editing, supervision.

Wim Janssens: Supervision, validation, review & editing, supervision.

Bart M. Vanaudenaerde: Supervision, study design, funding acquisition, resources, data curation, validation, review & editing.

All authors have read and approved the final version of the manuscript.

#### Data sharing statement

All data reported in this paper and source code will be made available upon request to the corresponding author.

#### Declaration of interests

BMV, WJ, WW, GGR are supported by the KU Leuven (C16/19/005).

LJC received a grant and consulting fees from Medtronic, MSC received payment or honoraria to the institution from Vertex Pharmaceuticals and is an unpaid member of the advisory board on PCDRResearch.org.

VG, CH, IG, PK, MV, XJ and JV are junior research fellows and RV is a senior research fellow supported by the Research Foundation Flanders (11L9824N, 1152225N, 11N3922N, 1120425N, 1SE4322N, 11PGT24N,1803521N, 1160025N). MV received compensation from Sanofi for attending ERS2023 congress.

SE received grants from Chiesi, consulting fees from GSK, payments or honoraria from GSK, Chiesi, Astra Zeneca and ALK and support for attending meetings from GSK, Sanofi and Astra Zeneca.

JJ declares funding from the Wellcome Trust, Gilead, Microsoft Research, GSK, Cancer Research UK, Rosetrees Trust and Cystic Fibrosis trust; consulting fees from Boehringer Ingelheim, Roche, GSK, NHSX; payment for honoraria received from Boehringer Ingelheim, Roche, GlaxoSmithKline, Takeda; support for attending meetings and/or travel from Boehringer Ingelheim; patents planned, issued or pending (UK patent application number 2113765.8 and UK patent application number GB2211487.0); participation on a Data Safety Monitoring Board or Advisory Board for Boehringer Ingelheim and Roche.

#### Acknowledgements

This research was funded by the KU Leuven grant (C16/19/005) received by BMV, WJ, WW, GGR.

#### Appendix A. Supplementary data

Supplementary data related to this article can be found at <https://doi.org/10.1016/j.ebiom.2025.105670>.

#### References

- Chen S, Kuhn M, Prettner K, et al. The global economic burden of chronic obstructive pulmonary disease for 204 countries and territories in 2020–50: a health-augmented macroeconomic modelling study. *Lancet Glob Health*. 2023;11:e1183–e1193.
- Agustí A, Celli BR, Criner GJ, et al. Global initiative for chronic obstructive lung disease 2023 report: GOLD executive summary. *Eur Respir J*. 2023;61:2300239.
- Hogg JC, Chu F, Utokaparch S, et al. The nature of small-airway obstruction in chronic obstructive pulmonary disease. *N Engl J Med*. 2004;350:2645–2653.
- Weibel ER. *Morphometry of the human lung*. Berlin, Heidelberg: Springer Berlin Heidelberg; 1963. <https://doi.org/10.1007/978-3-642-87553-3>.
- Pedley TJ, Schroter RC, Sudlow MF. The prediction of pressure drop and variation of resistance within the human bronchial airways. *Respir Physiol*. 1970;9:387–405.
- Horsfield K, Cumming G. Morphology of the bronchial tree in man. *J Appl Physiol*. 1968;24:373–383.
- Macklem PT, Mead J. Resistance of central and peripheral airways measured by a retrograde catheter. *J Appl Physiol*. 1967;22:395–401.
- Mead J. The lung's quiet zone. *N Engl J Med*. 1970;282:1318–1319.
- Hogg JC, Macklem PT, Thurlbeck WM. Site and nature of airway obstruction in chronic obstructive lung disease. *N Engl J Med*. 1968;278:1355–1360.
- Van Brabant H, Cauberghs M, Verbeken E, Moerman P, Lauweryns JM, Van De Woestijne KP. Partitioning of pulmonary impedance in excised human and canine lungs. *J Appl Physiol*. 1983;55:1733–1742.
- Yanai M, Sekizawa K, Ohru T, Sasaki H, Takishima T. Site of airway obstruction in pulmonary disease: direct measurement of intrabronchial pressure. *J Appl Physiol*. 1992;72:1016–1023.

- 12 McDonough JE, Yuan R, Suzuki M, et al. Small-airway obstruction and emphysema in chronic obstructive pulmonary disease. *N Engl J Med*. 2011;365:1567–1575.
- 13 Zhao Y, Lieber BB. Steady inspiratory flow in a model symmetric bifurcation. *J Biomech Eng*. 1994;116:488–496.
- 14 Nowak N, Kakade PP, Annapragada AV. Computational fluid dynamics simulation of airflow and aerosol deposition in human lungs. *Ann Biomed Eng*. 2003;31:374–390.
- 15 Freitas RK, Schröder W. Numerical investigation of the three-dimensional flow in a human lung model. *J Biomech*. 2008;41:2446–2457.
- 16 Mauroy B, Filoche M, Weibel ER, Sapoval B. An optimal bronchial tree may be dangerous. *Nature*. 2004;427:633–636.
- 17 Pfitzner J. Poiseuille and his law. *Anaesthesia*. 1976;31:273–275.
- 18 Yushkevich PA, Piven J, Hazlett HC, et al. User-guided 3D active contour segmentation of anatomical structures: significantly improved efficiency and reliability. *NeuroImage*. 2006;31:1116–1128.
- 19 Boon M, Verleden SE, Bosch B, et al. Morphometric analysis of explant lungs in cystic Fibrosis. *Am J Respir Crit Care Med*. 2016;193:516–526.
- 20 *Microfluidics: modelling, mechanics and mathematics*. Elsevier; 2017. <https://doi.org/10.1016/C2012-0-02230-2>.
- 21 Janna WS. *Introduction to fluid mechanics, 0 edn*. CRC Press; 2009. <https://doi.org/10.1201/9781420085259>.
- 22 Koo H-K, Vasilescu DM, Booth S, et al. Small airways disease in mild and moderate chronic obstructive pulmonary disease: a cross-sectional study. *Lancet Respir Med*. 2018;6:591–602.
- 23 Matsuba K, Thurlbeck WM. The number and dimensions of small airways in emphysematous lungs. *Am J Pathol*. 1972;67:265–275.
- 24 Nucci G, Suki B, Lutchen K. Modeling airflow-related shear stress during heterogeneous constriction and mechanical ventilation. *J Appl Physiol*. 2003;95:348–356.
- 25 Bilek AM, Dee KC, Gaver DP. Mechanisms of surface-tension-induced epithelial cell damage in a model of pulmonary airway reopening. *J Appl Physiol*. 2003;94:770–783.
- 26 Espina JA, Cordeiro MH, Milivojevic M, Pajić-Lijaković I, Barriga EH. Response of cells and tissues to shear stress. *J Cell Sci*. 2023;136:jcs260985.
- 27 Noskovicova N, Hinz B, Pakshir P. Implant Fibrosis and the underappreciated role of myofibroblasts in the foreign body reaction. *Cells*. 2021;10:1794.
- 28 Henderson NC, Rieder F, Wynn TA. Fibrosis: from mechanisms to medicines. *Nature*. 2020;587:555–566.
- 29 Polosukhin VV, Gutor SS, Du R-H, et al. Small airway determinants of airflow limitation in chronic obstructive pulmonary disease. *Thorax*. 2021;76:1079–1088.
- 30 Booth S, Hsieh A, Mostaco-Guidolin L, et al. A single-cell atlas of small airway disease in chronic obstructive pulmonary disease: a cross-sectional study. *Am J Respir Crit Care Med*. 2023;208:472–486.